

Numerical Investigation of Coupled Electrodynamic Tether / Electrostatic Propulsion Systems

IEPC-2007-107

*Presented at the 30th International Electric Propulsion Conference, Florence, Italy
September 17-20, 2007*

Torsten Stindl* and Markus Fertig†

Institut für Raumfahrtsysteme, Universität Stuttgart, 70550 Stuttgart, Germany

and

Monika Auweter-Kurtz‡

Universität Hamburg, 20146 Hamburg, Germany

To assess the feasibility of a coupled electrodynamic tether / electrostatic propulsion system (CETEP) under different conditions, numerical investigations are conducted at the Institut für Raumfahrtsysteme (Institute of Space Systems, IRS) of the Universität Stuttgart. CETEP has been proposed by the European Space Agency (ESA) in order to overcome the limitations of traditional electrodynamic tether systems with respect to attainable thrust levels and dependence from local plasma conditions in the ionosphere. A three-dimensional Particle in Cell (PIC) approach is used to simulate the particles in the vicinity of the tether system. The PIC scheme is part of a numerical method which is jointly developed by IRS, IAG (Institute of Aerodynamics and Gas Dynamics, Universität Stuttgart), HLRS (High Performance Computing Center Stuttgart) and IHM (Institute of Pulsed Power and Microwave Technology, Forschungszentrum Karlsruhe in der Helmholtz-Gemeinschaft) in order to approximately solve the Boltzmann equation for rarefied, non-continuum plasma flows. The modeling concept and methods are described and validation test results are reported.

Nomenclature

\vec{A}	vector potential
\vec{B}	magnetic induction
\vec{E}	electric field
\vec{j}	current density
l	length
\vec{n}	cell side normal
Q	charge
\vec{r}	vector between two points
S	cell side area
\vec{v}	velocity

Symbols

ϵ_0	electric permittivity
μ_0	magnetic permeability

*Scientist, Raumtransporttechnologie, stindl@irs.uni-stuttgart.de

†Head of Plasma Modeling and Simulation Group, Raumtransporttechnologie, fertig@irs.uni-stuttgart.de

‡Professor, President of the University of Hamburg, praesidentin@uni-hamburg.de

ϕ	electric potential
ρ	charge density
c	speed of light
ESA	European Space Agency
HLRS	Höchstleistungsrechenzentrum Stuttgart (High Performance Computing Center Stuttgart)
IAG	Institut für Aerodynamik und Gasdynamik (Institute of Aerodynamics and Gasdynamics)
IHM	Institut für Hochleistungsimpuls und Mikrowellentechnik (Institute of High Power Impulse and Microwave Technology)
IRS	Institut für Raumfahrtssysteme (Institute of Space Systems)
PIC	Particle in Cell
CETEP	Coupled Electrodynamic Tether / Electrostatic Propulsion

I. Introduction

A traditional electrodynamic tether generates thrust by driving a current through a several kilometers long, conducting wire extended from a spacecraft orbiting a celestial body with a magnetic field, e. g. Earth. The current interacts with the magnetic field and the resulting Lorentz force generates thrust for the spacecraft at the expense of electrical energy. Since the movement of the tether induces a voltage in the opposite direction, the voltage driving the current has to be high enough to not only overcome the resistance of the wire but also the induced voltage, which can reach several hundred volts per kilometer. In contrast to other space propulsion systems, this technique requires no propellant and could be used for a multitude of applications, like space station orbit maintenance, satellite orbit boosts and the propulsion of planetary probes.

The thrust generated by such an electrodynamic tether system is proportional to the current driven through the tether and the magnetic field strength. Since no closed circuit exists, the electrons forming the tether current have to be acquired externally. This can be achieved by collecting electrons from the surrounding ionosphere at one end of the tether and emitting them at the other end. Therefore, the possible current and thrust are highly dependent on the ability to extract the electrons from the ionospheric plasma. One way to collect electrons is by using a passive, biased metallic sphere as an anode. This method was tested on board the TSS-1R (Tethered Satellite System). While the collected current exceeded the one predicted by the standard Parker-Murphy model, which takes into account the dominant magnetic effects, only about 0.35 A at a bias of about 1 kV were reached.¹ This indicates that a voltage of approximately 35 kV is needed to reach e. g. 2 A in the same ionospheric conditions which would translate into a requirement of 70 kW for a thrust of 0.3 N with a 10 km tether in a Low Earth Orbit.² Additionally, a spherical passive collector has the disadvantage of high aerodynamic drag.

Another way to collect the electrons is to use plasma contactors, such as hollow cathodes, as active anodes. The Plasma Motor Generator (PMG) experiment used an active anode, and reached 0.3 A under a 130 V bias and optimal conditions.¹ The current showed a strong dependence on ionospheric conditions with lower currents especially in the nighttime part of the orbit. Local electron density in the ionosphere fluctuates strongly (up to two orders of magnitude) with the time of day and e. g. sunspot activity, leading to unpredictable and highly dependent current collection abilities.

In order to increase the current driven through the tether and at the same time achieve a higher degree of independence from the local plasma conditions, it would be advantageous if the electrons were generated on board the spacecraft and directly driven through the tether without having to be collected from the plasma first.

This can be achieved by using an ion thruster to generate the electrons. Within an ion thruster, a propellant (e. g. Xenon) is ionized and the positively charged ions are emitted, retaining the electrons. The ions are accelerated by a negatively charged grid and provide the thrust while the electrons are emitted downstream into the ion beam by an electron source – the neutralizer – in order to prevent spacecraft charging. If an ion thruster is placed at one end of the tether and the neutralizer is placed at the other end, as depicted in Fig. 1, the neutralizing current flows through the tether and provides propulsion without the need to collect electrons from the surrounding plasma. The current is equivalent to the ion thruster's beam current, therefore reaching about 3-4 A or more, depending on the thruster type and number of thrusters

used. If the ion thruster emits in the appropriate direction it also contributes to the thrust generated by the system. As with a traditional electrodynamic tether, additional power would be required to drive the increased current through the tether. This so-called coupled electrodynamic tether / electric propulsion (CETEP) system was proposed by ESA.²

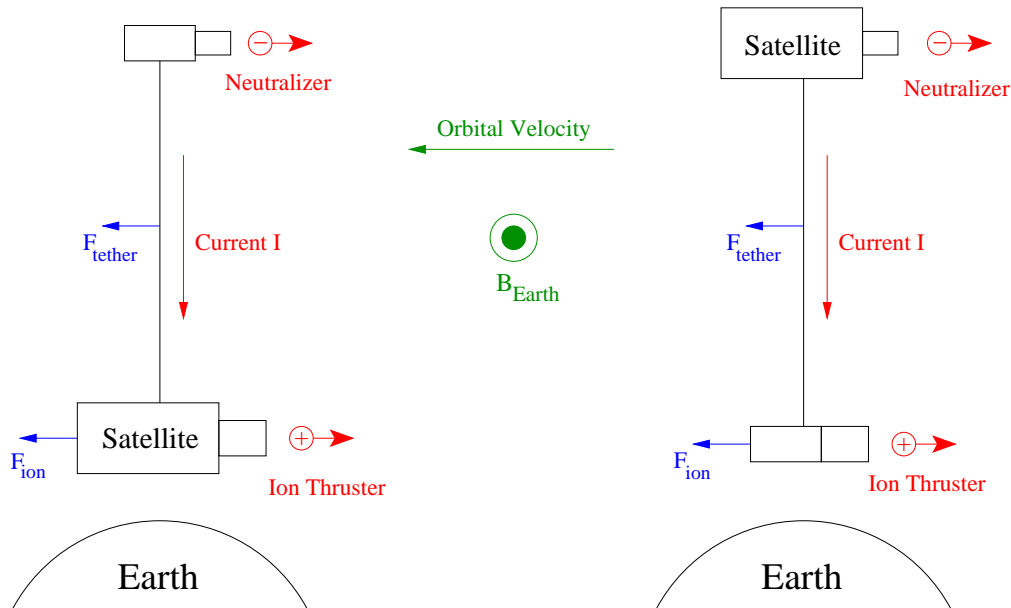


Figure 1. CETEP operating principle: Neutralizer deployed (left) or on the satellite (right)

While such a system is feasible in theory, it has never been tested. Therefore, the behavior of electrons and ions after leaving the neutralizer and the thruster is being studied at the Institut für Raumfahrtssysteme (IRS) at the Universität Stuttgart using a numerical particle approach. The interaction of emitted particles with each other and with the external electromagnetic fields, the tether itself, the surrounding conditions (like Earth's magnetic field) and the electron and ion sources will be modeled to study the functioning and feasibility of a CETEP system.

A cooperation between IRS, IAG (Institute of Aerodynamics and Gas Dynamics, Universität Stuttgart), HLRS (High Performance Computing Center Stuttgart) and IHM (Institute of Pulsed Power and Microwave Technology, Forschungszentrum Karlsruhe in der Helmholtz-Gemeinschaft) has been formed in order to develop a hybrid particle scheme for approximately solving the Boltzmann equation for rarefied and reactive plasmas.³ This scheme will include collisions and short range coulomb interactions between particles which will be neglected in the case of the CETEP system due to the low particle densities encountered. If necessary, they will be included at a later point in the study, though. The need for a three-dimensional description and the large computational domain require optimization and parallelization of the code in order to effectively use high performance computer systems.

II. Modeling

Due to the low densities, no continuous velocity distribution function can be assumed. Therefore, a particle based approach is being used. A typical ion flux of an ion thruster is about 10^{19} s^{-1} . Since the computational domain for CETEP has to be very large, the number of ions to be simulated is at least 10^{15} . Even with the fastest currently available computer systems it is not feasible to simulate every physical particle. Therefore, so-called macro particles are simulated, where each macro particle represents a user defined number of physical particles.

The magnetic field induced by the tether current has an effect on the emitted particles as well as on the particles in the ionosphere, especially the lighter electrons. Also, the particles emitted by the neutralizer and the ion thruster interact with each other, so that it is essential to not only consider the external fields but also the fields generated by the particles themselves.

The type of neutralizer, i.e. the method of emitting electrons, is expected to heavily influence the possible development of a space charge near the neutralizer. Electrons can be emitted non-directionally or uni-directionally. Also, it should theoretically be possible to employ a second ion thruster as “neutralizer”. This second ion thruster would generate thrust using negative ions, thereby emitting the excess electrons from the first ion thruster. Due to their higher mass and velocity, ions are influenced less by the various electromagnetic fields and therefore are less inclined to form a charge cloud.

The environment in a Low Earth Orbit has additional effects on the emitted ions and electrons. Earth’s magnetic field exerts a $j \times B$ Lorentz force on the particles and the local plasma generates additional local electromagnetic fields. It has to be determined whether these have an influence on the performance of CETEP and need to be modeled as well.

To simulate the particle behavior, a Particle-in-Cell (PIC) approach is used. Within a PIC scheme, particle movement and the self-consistent determination of the local electric and magnetic fields are decoupled. Figure 2 shows the iteration of one time step of a PIC scheme. Given a particle distribution within the computational domain, the charge and current densities define the electromagnetic eigenfields. Therefore, their values at the particle positions have to be assigned to node or cell values on a computational grid for the field solver, where they act as source terms. This field solver is the essential step of the PIC scheme and the focus of the present work. It computes the \vec{E} - and \vec{B} -fields in the cells, after which they have to be evaluated at the particle positions to determine the Lorentz forces acting on the charged particles. Hence, the field values have to be extrapolated from grid positions to particle positions with the desired order of accuracy. The Lorentz solver then determines the acceleration of the particles. Afterwards, they are moved in a separate pushing step. At this point, other parts of the jointly developed scheme can contribute additional accelerations due to e.g. collisions. The particles are advanced using the usual laws of dynamics, taking into account relativistic effects. Within a combined routine, applicable particle boundary conditions (e.g. removal or reflection) are considered and the particles are localized on the grid. This yields the new particle distribution on the grid as the starting point for the next cycle.

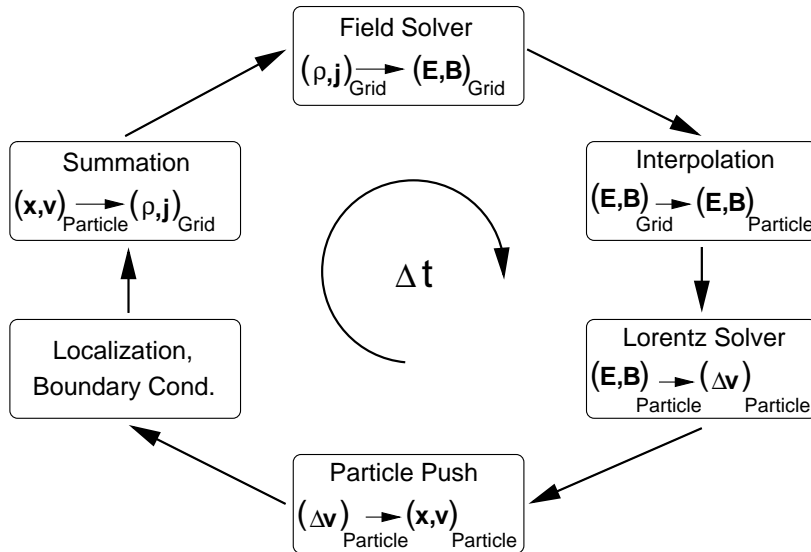


Figure 2. Particle-in-Cell time step cycle

III. Field Solvers

According to the law of dynamics for charged particles, the force \vec{F} on a given particle with the charge q and the velocity \vec{v} is determined by the Lorentz force and depends on the electric field \vec{E} and the magnetic induction \vec{B} :

$$\vec{F} = q[\vec{E} + \vec{v} \times \vec{B}]. \quad (1)$$

The difficulties in employing the Lorentz equations arise from the fact that the electric field \vec{E} and the magnetic induction \vec{B} are not given explicitly. They have to be calculated at each time step from Maxwell's equations

$$\frac{\partial \vec{E}}{\partial t} - c^2 \nabla \times \vec{B} = -\frac{\vec{j}}{\epsilon_0}, \quad (2)$$

$$\frac{\partial \vec{B}}{\partial t} + \nabla \times \vec{E} = 0, \quad (3)$$

$$\nabla \cdot \vec{E} = \frac{\rho}{\epsilon_0}, \quad (4)$$

$$\nabla \cdot \vec{B} = 0, \quad (5)$$

where the electric permittivity ϵ_0 and magnetic permeability μ_0 are related to the speed of light c according to $\epsilon_0 \mu_0 c^2 = 1$. For given charge and current densities ρ and \vec{j} , Maxwell's equations describe the temporal and spatial evolution of the electric field \vec{E} and the magnetic induction \vec{B} .

Two methods of obtaining these electromagnetic fields from the particle distribution have been implemented and will be presented here. Both methods are finite volume schemes on unstructured grids. While they show promising results in preliminary tests (see section IV), further investigations are necessary in order to validate and verify them for the simulation of CETEP.

A. Maxwell Solver

The divergence constraints (4) and (5) are automatically satisfied for all times if the initial values satisfy these relations. Therefore, it would be sufficient to solve the hyperbolic evolution equations (2) and (3) only.

Unfortunately, numerical errors may occur in the simulation, leading to small errors being introduced at each time step. If only the hyperbolic evolution equations are numerically solved, then these errors may increase and strongly falsify the solution. For a self-consistent movement of charged particles, Eqs. (4) and (5) have to be coupled with Eqs. (2) and (3). In the Generalized Lagrange Multiplier approach,⁴ two additional variables $\Phi(\vec{x}, t)$ and $\Psi(\vec{x}, t)$ are introduced into Maxwell's equations to couple the equations. The coupling terms may be chosen such that a purely hyperbolic system can be formed. If the errors are zero, then it coincides with the original Maxwell's equations. The Purely Hyperbolic Maxwell (PHM) equations system then reads as

$$\frac{\partial \vec{E}}{\partial t} - c^2 \nabla \times \vec{B} + \chi c^2 \nabla \Phi = -\frac{\vec{j}}{\epsilon_0}, \quad (6)$$

$$\frac{\partial \vec{B}}{\partial t} + \nabla \times \vec{E} + \gamma \nabla \Psi = 0, \quad (7)$$

$$\nabla \cdot \vec{E} + \frac{1}{\chi} \frac{\partial \Phi}{\partial t} = \frac{\rho}{\epsilon_0}, \quad (8)$$

$$\nabla \cdot \vec{B} + \frac{1}{\gamma c^2} \frac{\partial \Psi}{\partial t} = 0, \quad (9)$$

where the dimensionless positive parameters χ and γ represent the transportation coefficients for the local errors Φ and Ψ . These new variables $\Phi(\vec{x}, t)$ and $\Psi(\vec{x}, t)$ define two additional degrees of freedom and, as mentioned above, couple the divergence conditions (4), (5) to the evolution equations (2), (3).

This correction technique ensures that divergence errors within the electromagnetic PIC computation cannot increase and falsify the numerical simulation results. The method has already been described in detail⁴⁻⁶ and is only presented here in order to provide a comparison to the solver described below.

B. Poisson Solver

A significant disadvantage of the Maxwell solver described in the last section is that the time step usually is very small since the fields expand at the velocity of light. This requires that within one time step the field can at most move a fraction of the cell size, resulting in time steps of e. g. about 10^{-12} s for cell

dimensions of about 1 cm. This leads to a huge number of iteration steps for problems with a larger time frame. Therefore, the method is feasible for problems with a short duration or small dimensions, like the simulation of a pulsed plasma thruster,³ but less so for the simulation of CETEP. Additionally, in the case of CETEP, the stationary solution is of interest and the speed of the simulated particles is assumed to be low in comparison to the speed of light. Hence, the time dependent parts of the Maxwell equations can be neglected. Introducing the electric potential ϕ with

$$\vec{E} = -\nabla\phi \quad (10)$$

and the magnetic vector potential \vec{A} with

$$\vec{B} = \nabla \times \vec{A} \quad (11)$$

leads to Poisson's equations

$$\nabla^2\phi = -\frac{\rho}{\epsilon_0} \quad \text{and} \quad \nabla^2\vec{A} = -\mu_0\vec{j}, \quad (12)$$

where the three components of \vec{A} and \vec{j} are decoupled and can be written as three separate Poisson equations:

$$\nabla^2 A_{x,y,z} = -\mu_0 j_{x,y,z} \quad (13)$$

In order to solve these equations, a finite volume approach is used. Integration of Eq. (12) over the volume of a cell yields

$$\int_V \nabla^2\phi \, dV = \int_V -\frac{\rho}{\epsilon_0} \, dV. \quad (14)$$

With Gauss's Law, the left hand side can be written as

$$\int_V \nabla^2\phi \, dV = \int_V \nabla \cdot \nabla\phi \, dV = \oint_S \nabla\phi \cdot \vec{n} \, dS, \quad (15)$$

where S is the surface of the element and \vec{n} the normal of the surface pointing outwards. Numerical approximation on a tetrahedron i (see Fig. 3) leads to

$$\sum_j \nabla\phi_{i,j} \cdot \vec{n}_{i,j} S_{i,j} = -\frac{Q_i}{\epsilon_0} \quad (16)$$

for the four sides j , where Q_i is the charge of the particles within the cell i and $\phi_{i,j}$ denotes the gradient of ϕ at the sides of the cell.

The direct determination of these gradients is costly on unstructured grids. According to Blazek,⁷ the gradient at a cell side $\nabla\phi_{i,k}$ can be computed from the gradients of the two neighboring cells $\nabla\phi_i$ and $\nabla\phi_k$ using the relation

$$\nabla\phi_{i,k} = \overline{\nabla\phi}_{i,k} - [\overline{\nabla\phi}_{i,k} \cdot \vec{r}_{i,k} - (\frac{\phi_k - \phi_i}{l_{i,k}})] \vec{r}_{i,k}, \quad (17)$$

where $\vec{r}_{i,k}$ is the unit vector from the center of cell i to the center of cell k and $l_{i,k}$ is the distance between the cell centers. $\overline{\nabla\phi}_{i,k}$ denotes the mathematical average of the gradients in the cell centers,

$$\overline{\nabla\phi}_{i,k} = \frac{1}{2}(\nabla\phi_i + \nabla\phi_k). \quad (18)$$

To determine the gradients $\nabla\phi_i$ and $\nabla\phi_k$, a linear ansatz including the adjacent cell centers could be used with a least squares approach to solve the resulting overdetermined system.

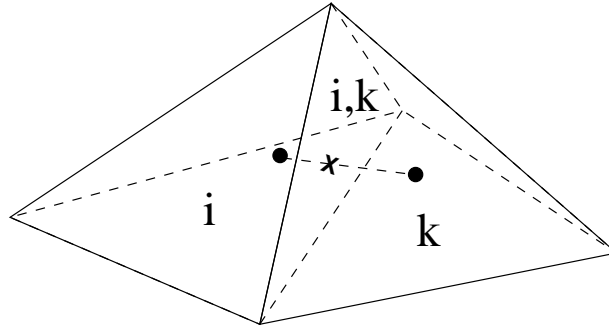


Figure 3. Gradient at i,k: The cross marks the location where the gradient at the side between the tetrahedrons i and k is evaluated.

Howere, using the Voronoi dual of the Delaunay triangulation, a significantly less costly approach is possible. On a Delaunay grid, no node of the grid is allowed to be inside the circumsphere of any tetrahedron. The circumcenters of the tetrahedrons can then be connected to form the so-called Voronoi cells. Figure 4 shows this concept for the two-dimensional case. A Voronoi cell contains all the points closest to a node and the sides of the cells are always orthogonal to the grid edges connecting the nodes. Following Gatsonis and Spirkin,⁸ this orthogonality leads to

$$\nabla\phi_{i,k} \cdot \vec{n}_{i,k} = \frac{\phi_k - \phi_i}{l_{i,k}}, \quad (19)$$

where i and k denote the Voronoi cells corresponding to the nodes of the original tetrahedral grid. Equation (16) can then directly be written as

$$\sum_k (\phi_k - \phi_i) \frac{S_{i,k}}{l_{i,k}} = -\frac{Q_i}{\epsilon_0}, \quad (20)$$

shifting the finite volume approach from the tetrahedral cells to the Voronoi cells. The disadvantage of this approach is that only meshes with the Delaunay triangulation can be used. Since the computational domain for CETEP in space has no geometrically defined borders such as walls, it is expected that a Delaunay grid can always be constructed. This needs to be investigated further, though, especially with regard to local grid refinement.

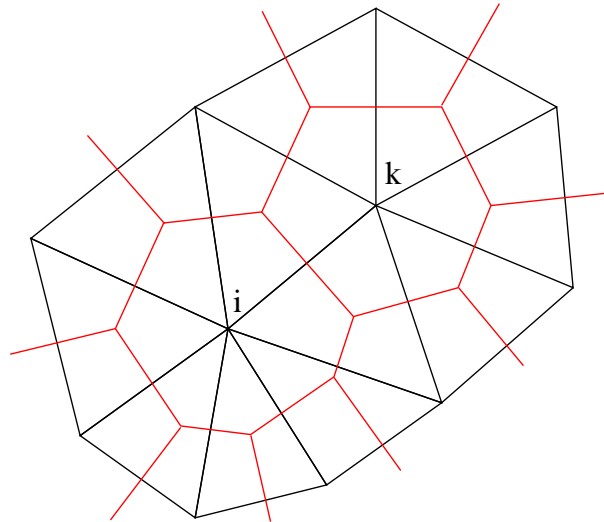


Figure 4. Voronoi Cells (in red) at the nodes of a triangular mesh obtained by connecting the circumcenters of the triangles. The faces of the voronoi cells are then orthogonal to the sides of the triangles and halve them. In the three-dimensional case, the same approach is used on tetrahedrons.

Evaluation of Eq. (20) at each node yields the linear equation system

$$\mathbf{M} \cdot \begin{pmatrix} \phi_1 \\ \phi_2 \\ \dots \\ \phi_N \end{pmatrix} = \frac{1}{\epsilon_0} \begin{pmatrix} Q_1 \\ Q_2 \\ \dots \\ Q_N \end{pmatrix} \quad (21)$$

with the sparsely populated matrix \mathbf{M} . This equation system has the standard $A \cdot x = b$ format and is solved using a suitable equation system solver. To calculate the vector potential \vec{A} , the same principles are applied to each of the three components of \vec{A} . As long as the grid is the same for ϕ and \vec{A} , the matrix \mathbf{M} is equal for the potential and the three vector potential components, which significantly speeds up calculation.

The \vec{E} and \vec{B} fields are calculated from the (vector) potential using a linear least squares approach. The now known values for ϕ , A_x , A_y and A_z at each node and its neighboring nodes are used to compute their gradients at the node. From these gradients, the fields can be derived directly using Eqs. (10) and (11).

Currently, only Dirichlet boundary conditions are implemented for the Poisson Solver. The given potential is directly applied to the boundary nodes and the resulting factor is added to the right-hand side of Eq. (21). Other boundary conditions, e. g. the extrapolation of potential values from the grid towards the boundary or Neumann conditions, are possible and will be implemented as the need arises.

IV. Validation Results

Since the PIC method decouples particle movement and field computation, they can be investigated separately. In order to validate the code, the numerical solution of a given test case has to be compared to the analytical solution. To be able to obtain such an analytical solution, test cases with only one or two macro particles have been chosen, which allows validation of the methods on a basic level.

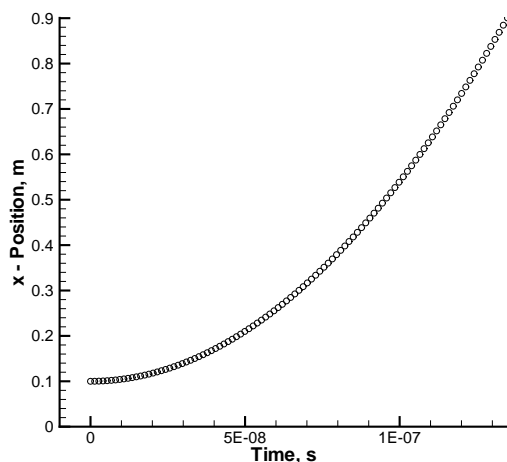


Figure 5. Movement of an electron within a constant electric field in x-direction.

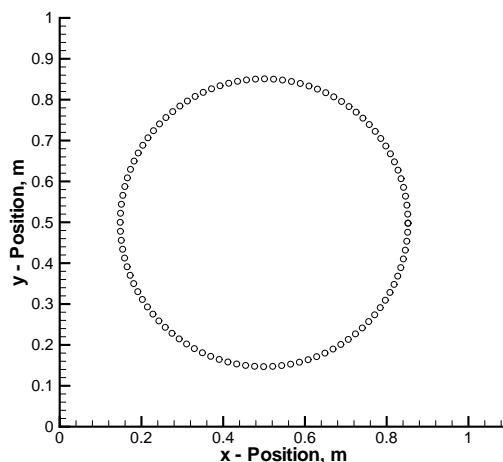


Figure 6. Movement of an electron within a constant magnetic field in z-direction.

Lorentz Solver and Particle Movement: To validate the particle movement due to the Lorentz force, the motion of a single particle within constant, homogeneous electromagnetic fields is compared to the analytically calculated motion. Accelerating a particle by an external electric field of 500 V/m in x-direction results in the parabola in Fig. 5, depicting the position of the particle over time. Applying an external magnetic field to a moving particle results in a circular motion in the plane orthogonal to the magnetic field. Figure 6 shows such a motion in a constant field of about $16 \cdot 10^{-6}$ T in z-direction and a particle velocity of 10^6 m/s. In Fig. 7, the L2 error norm of the movement is plotted against time step size, which is chosen

proportional to the grid cell size, showing that the particle movement is of second order accuracy due to the currently implemented leapfrog-scheme introduced by Boris.⁹

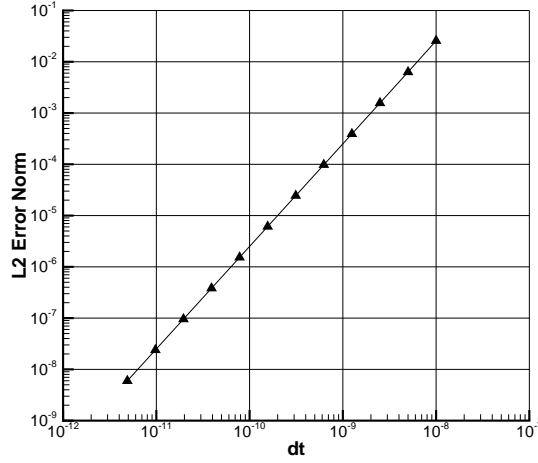


Figure 7. L2 error norm for different time step sizes dt [s], depicting second order accuracy

Field Solver: The validation of the Maxwell solver has already been discussed in previous works.^{5,6} In order to validate the Poisson field solver, the fields generated by a single (macro) particle are compared to their analytical solutions. In the following examples, a macro particle consisting of 10^{10} electrons is placed in the center of the computational domain at (0.5,0.5,0.5) with a velocity of 10^7 m/s in y-direction. The potential generated by a the particle at an arbitrary point is calculated with

$$\phi(\vec{r}) = \frac{1}{4\pi\epsilon_0} \cdot \frac{Q}{|\vec{r}|}, \quad (22)$$

where \vec{r} is the vector from the particle to the point and Q is the charge of the particle. Figure 8 depicts the computed potential in comparison to the analytical solution. Note that the values inside a cell are not interpolated, i. e. constant, resulting in the steps in the potential. At the particle position itself, a singularity exists, which cannot be resolved by the solver. The electric field of the particle at a given point then is

$$\vec{E}(\vec{r}) = \frac{1}{4\pi\epsilon_0} \cdot \frac{Q}{|\vec{r}|^2} \cdot \frac{\vec{r}}{|\vec{r}|}. \quad (23)$$

Figure 9 shows the E_x -field along a line in x-direction through the particle position. Close to the singularity, the error of the solver increases due to the increasing gradient of the potential. At the particle position itself, the field vanishes so that the particle theoretically is not accelerated by its own field. Practically, numerical errors prevent the field from being exactly zero at the particle position, so a small acceleration is always present. This error scales with the charge of the particle, possibly leading to problems with extremely large macro particle factors. Since the fields of all other particles scale at the same rate, though, this should not pose a problem in simulations with a multitude of particles. Also, the field at the particle position is of the same order of accuracy as in the rest of the domain and decreases with decreasing cell sizes. Comparing the B_z -field along a line in y-direction with the analytical solution

$$\vec{B}(\vec{r}) = \frac{\mu_0}{4\pi} \cdot \frac{Q(\vec{v} \times \vec{r}/|\vec{r}|)}{|\vec{r}|^2} \cdot \frac{\vec{r}}{|\vec{r}|}. \quad (24)$$

yields Fig. 10. It shows the same behavior regarding the errors at the particle position and close to the singularity as the electric field.

Complete Solver: In order to validate the coupling of the field solver and the particle movement, the circular motion of an electron around a proton is simulated. Due to its larger mass, the proton is basically

motionless and its electric field forces the electron into an orbit. Equating the Lorentz force and the centrifugal force, the electron velocity for a circular orbit can be calculated. In the example shown in Fig. 11, the velocity is about 28 km/s with a radius of 0.32 m and a proton macro particle factor of 10^{10} .

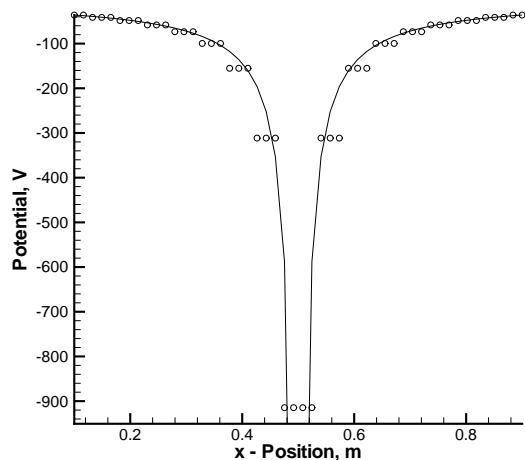


Figure 8. Electric potential ϕ of an electron macro particle (points) in comparison to the analytical solution (line).

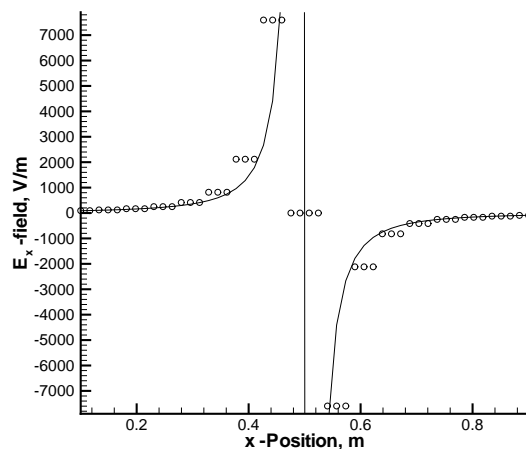


Figure 9. E_x field of an electron macro particle (points) in comparison to the analytical solution (line).

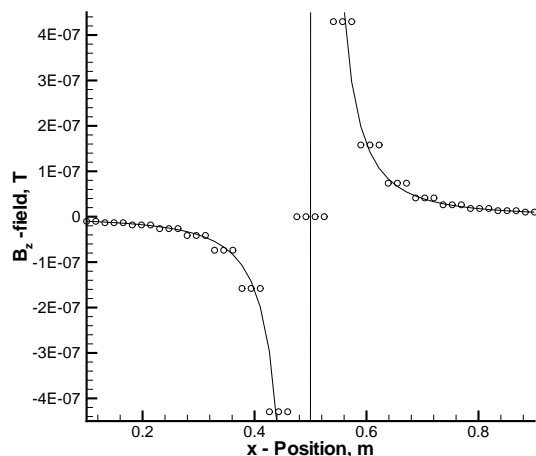


Figure 10. B_z field of an electron macro particle (points) in comparison to the analytical solution (line).

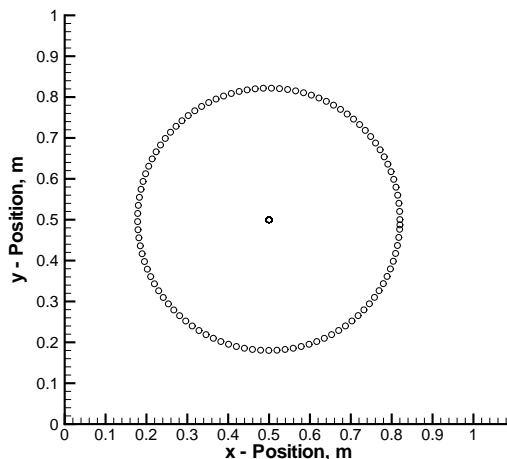


Figure 11. Electron circling a proton macro particle due to its electric field.

V. Summary and Outlook

In order to assess the feasibility of coupled electrodynamic tether / electric propulsion systems, they are being investigated numerically at the IRS. A PIC scheme is used to compute the movement of particles depending on their self-fields and external fields. Since a direct simulation of all ions and electrons present in the vicinity of the tether is far from being possible, macro particles are used, with each macro particle representing a number of physical particles. Different field solvers have been implemented and validated by comparison with the analytical solution of basic test cases and the results have been reported. Further

investigations are necessary to ensure correct results on various grids and with larger problems. Preliminary investigations of small and increasingly larger CETEP systems will be conducted. The results of these tests will determine the approach to simulating large tether systems, especially considering the huge differences in scale and acceptable calculation times. The code will be parallelized and optimized in order to ensure efficient usage of high performance computers. Depending on the CETEP results, it might be necessary to refine or change the field solving methods, especially the interpolation from the fields to the particles needs to be addressed for larger cell sizes. Similarly, the other parts of the scheme will be improved and refined, partly in cooperation with our partners.

Acknowledgments

Torsten Stindl thanks the Landesgraduiertenförderung Baden-Württemberg and the Erich-Becker-Stiftung, Germany, for their financial support.

References

- ¹Cosmo, M. and Lorenzini, E., "Tethers in Space Handbook," The Smithsonian Astrophysical Observatory, Cambridge, Third Edition, 1997.
- ²Nicolini, D. and Ockels, W., "Coupled Electrodynamic Tether/ Electrostatic Propulsion System," International Electric Propulsion Conference, Toulouse, France, 2003.
- ³Petkow, D., Fertig, M., Stindl, T., Auweter-Kurtz, M., Quandt, M., Munz, C.-D., Roller, S., D'Andrea, D., and Schneider, R., "Development of a 3-Dimensional, Time Accurate Particle Method for Rarefied Plasma Flows," AIAA-2006-3601, Proceedings of the 9th AIAA/ASME Joint Thermophysics and Heat Transfer Conference, San Francisco, USA, 2006.
- ⁴Munz, C.-D., Omnes, P., and Schneider, R., "A three-dimensional finite-volume solver for the Maxwell equations with divergence cleaning on unstructured meshes," *Computer Physics Communications*, Vol. 130, 2000, pp. 83 – 117.
- ⁵Auweter-Kurtz, M., Fertig, M., Petkow, D., Stindl, T., Quandt, M., Munz, C.-D., Adamis, P., Resch, M., Roller, S., D'Andrea, D., and Schneider, R., "Development of a hybrid PIC/DSMC Code," IEPC-2005-71, Proceedings of the 29th International Electric Propulsion Conference, Princeton, USA, 2005.
- ⁶Stindl, T., Fertig, M., and Auweter-Kurtz, M., "Investigation of Coupled Electrodynamic Tether / Electrostatic Propulsion Systems Using a Particle Approach," AIAA-2006-4651, Proceedings of the 42nd AIAA/ASME/SAE/ASEE Joint Propulsion Conference and Exhibit, Sacramento, USA, 2006.
- ⁷Blazek, J., *Computational Fluid Dynamics: Principles and Applications*, Elsevier, Burlington, Massachusetts, 2001.
- ⁸Gatsonis, N. A. and Spirkin, A., "Unstructured 3D PIC Simulations of Field Emission Array Cathodes for Micropropulsion Applications," AIAA 2002-3678, Proceedings of the 38th AIAA/ASME/SAE/ASEE Joint Propulsion Conference and Exhibit, Indianapolis, USA, 2002.
- ⁹Boris, J. P., "Relativistic Plasma Simulations – Optimization of a Hybrid Code," *Proc. 4th Conf. on Num. Sim. of Plasmas*, NRL Washington, Washington DC, 1970, pp. 3–67.